Electron-positron pair creation induced by two sequential short pulses

X. X. Zhou [1] C. K. Li [1] N. S. Lin,[2,*] and Y. J. Li[1,2,†]

[1]*State Key Laboratory for Geomechanics and Deep Underground Engineering,*
China University of Mining and Technology, Beijing 100083, China
[2]*School of Science, China University of Mining and Technology, Beijing 100083, China*

The computational quantum field theory (CQFT) is applied to study the dependence of the total EPP number on the time interval under the spatially localized double cosine-Gaussian pulse and the alternating-sign double-Gaussian pulse. The total EPP number damply oscillates with the time interval, and the oscillation frequency is about the energy gap ($2mc^2$) for all of the scenarios. This characteristic oscillation of the total EPP number is consistent with a formula, which is related to the amplitude mode in the BCS superconductors. Besides, we find that the Ramsey interference effect is not responsible for the characteristic oscillation by studying the double-Gaussian pulse with the same sign. Finally, when the favorable time interval is applied, the EPP number is much larger than the sum of the EPP number obtained in two single pulses. The favorable time interval mainly depends on the pulse duration and the carrier envelope phase (the quantity in cosine-Gaussian pulse).

I. INTRODUCTION

The vacuum of the quantum electrodynamics is unstable and can decay into the electron-positron pairs (EPPs) under the strong enough external field. In 1951, the EPP creation probability was calculated for a uniform electrostatic field by Schwinger [1]. The critical field strength in the Schwinger mechanism is $E_c = 10^{18}$ V/m, which is still unreachable nowadays. The electron-positron pairs can also be created by the nonlinear Breit-Wheeler process, which has been tested at the SLAC E-144 experiment [2]. In the experiment, the high-energy photons are generated by colliding the electron beam with a low-intensity laser (nonlinear compton scattering process), and then the high-energy photons collides with the laser to create the electron-positron pairs (nonlinear Breit-Wheeler process). Due to the participation of the electron beam, the pair creation at the SLAC experiment is not induced by pure laser light. In recent years, the development of the laser technology [3] stimulates the theoretical studies about the nonlinear Breit-Wheeler process in intense short laser pulses [4], which are usually simplified by the short electric pulses [5].

Theoretical studies mainly aim at enhancing the EPP creation probability or lowering the threshold of the EPP creation by studying the effects of the pulse parameters or constructing the external field configurations. The nonlinear Breit-Wheeler process induced by pure laser light might can be realized experimentally in the foreseeable future, with the guidance of the theoretical studies. Previous studies indicated that the EPP creation are sensitive to the details of the external field. On one hand, the EPP creation in a single pulse depends on the temporal pulse shape and the pulse parameters (i.e., the pulse strength, the pulse duration, or the CEP) [6–10]. On the other hand, the combination of several electric pulses in the external field configuration is not equivalent to the simple linear superposition of the action of each pulse. Some new effects may occur in the combination field, such as the interference effect in sequence of alternating-sign pulses, the enhancement effect in the superimposition of a strong and slow pulse with a weaker and fast pulse [11]. In addition, in the combination field, not only the pulse parameters of each pulse can affect the EPP creation, but the parameters between the pulses also can affect the EPP creation, such as the time interval between two adjacent pulses. The combination of two spatially homogeneous pulses with a time interval has been studied in some researches [12–16]. These researches mainly study the momentum distribution of the electrons or the positrons, and indicate that the momentum distribution is sensitive to the time interval. A few results about the dependence of the total EPP creation probability (W) on the time interval (δ) in Ref. [15]. The total EPP creation probability damply oscillates with the time interval in a nearly constant period. The peaks and valleys in the $W(\delta)$ curve manifest that the good value of the time interval can promote the EPP production probability, while the poor time interval suppresses the EPP creation. The sensitive dependence of the EPP creation probability on the time interval motivates us to make a further study. Since the temporal pulse shape [8–10] and the spatial distribution [17] of the electric field both can affect the EPP creation. In our work, the dependence of the total EPP number on the time interval is comprehensively studied under spatially localized double pulse. The spatial distribution of the electric field pulses are chosen as the Sauter electric field $E(x) = V_0/2W\{1 - [\tanh(x/W)]^2\}$, i.e., the pulse is confined to a region of size $2W$ along the x direction [21,22]. Furthermore, the double-Gaussian pulse and

*phy.nslin@gmail.com
†lyj@aphy.iphy.ac.cn

the double cosine-Gaussian pulse are both studied to distinguish whether the effect of the time interval depends on pulse shape. The cosine-Gaussian pulse has subcycle structure, and in which the turning points [6,12,18–20] are naturally exist, while the Gaussian pulse is monocycle.

The paper is organized as follows. In Sec. II, the computational quantum field theory (CQFT) is briefly introduced. In Sec. III, we study and discuss the dependence of the total EPP number on the time interval under several external fields, including the double cosine-Gaussian pulse, the alternating-sign double-Gaussian pulse, and the double-Gaussian pulse with the same sign. The effects of the pulse parameters (i.e., the pulse duration, the pulse strength, or the CEP) and the pulse shape are discussed. Furthermore, the dependence of the total EPP number on the time interval is fitted by a formula. The influence of the Ramsey interference effect on the dependence of the total EPP number on the time interval is studied as well. Finally, the EPP creation in double and single pulses is compared. In Sec. IV, we make a conclusion.

II. THE THEORETICAL FRAMEWORK

Let us first describe the main idea of the numerical method. To study the EPP creation process, the single particle quantum mechanical description is not sufficient and the quantum field theory is necessary to understand the particle creation and annihilation. In our model the external field is uniform in space except localized in the x axis, the time evolution of the quantum field operator $\hat{\Psi}(x, t)$ is described by the Dirac equation [23–27] (here and below we use the atomic unit).

$$i\frac{\partial}{\partial t}\hat{\psi}(x, t) = [c\sigma_1 p_x + \sigma_3 c^2 + V(x, t)]\hat{\psi}(x, t), \quad (1)$$

where σ_1 and σ_3 are the Pauli matrices. The electric field is described by the scalar potential $V(x, t)$. We focus on the x axis, and the Dirac four component spinor wave functions can be reduced to two (see, e.g., Refs. [26,27] for a more detailed introduction).

The field operator satisfies the Dirac equation as well as the time-dependent Heisenberg equation $i\partial\hat{\Psi}(t)/\partial t = [\hat{H}, \hat{\Psi}(t)]$ [27–29]. The corresponding quantum field theoretical Hamiltonian $\hat{H} = \hat{\Psi}^{\dagger}h\hat{H}$, where $h = c\sigma_1 p_x + \sigma_3 c^2 + V(x, t)$. The field operator can be expanded as

$$\hat{\psi}(x, t) = \sum_p \hat{b}_p(t)u_p(x) + \sum_n \hat{d}_n^{\dagger}(t)v_n(x)$$
$$= \sum_p \hat{b}_p u_p(x, t) + \sum_n \hat{d}_n^{\dagger} v_n(x, t), \quad (2)$$

where $\hat{b}_p$ and $\hat{d}_n^{\dagger}$ are the particle annihilation and the antiparticle creation operators, respectively. The subscripts p and n represent positive and negative energy, respectively. The field-free Hamiltonian $h_0 = c\sigma_1 p_x + \sigma_3 c^2$ at $t = 0$, and its energy eigenstates are $u_p(x)$ $(E \geqslant c^2)$ and $v_n(x)$ $(E \leqslant -c^2)$. $u_p(x, t)$ and $v_n(x, t)$ are respectively the time evolved eigenstates of $u_p(x)$ and $v_n(x)$, and their evolution satisfy the Dirac equation

[Eq. (1)]. The time evolution of the fermion annihilation and creation operators are

$$\hat{b}_p(t) = \sum_{p'} \hat{b}_{p'} \int dx u_p^*(x)u_{p'}(x, t)$$
$$+ \sum_{n'} \hat{d}_{n'}^{\dagger} \int dx u_p^*(x)v_{n'}(x, t), \quad (3)$$

$$\hat{d}_n^{\dagger}(t) = \sum_{p'} \hat{b}_{p'} \int dx v_n^*(x)u_{p'}(x, t)$$
$$+ \sum_{n'} \hat{d}_{n'}^{\dagger} \int dx v_n^*(x)v_{n'}(x, t), \quad (4)$$

respectively. The electronic portion of the field operator $\hat{\psi}_e(x, t) \equiv \sum_p \hat{b}_p(t)u_p(x)$, and the total number of the created EPPs is defined as

$$N(t) = \int dx \langle\!\langle \mathrm{vac} \| \hat{\psi}_e^{\dagger}(x, t)\hat{\psi}_e(x, t) \| \mathrm{vac} \rangle\!\rangle$$
$$= \sum_p \langle\!\langle \mathrm{vac} \| \hat{b}_p^{\dagger}(t)\hat{b}_p(t) \| \mathrm{vac} \rangle\!\rangle, \quad (5)$$

where $\| \mathrm{vac} \rangle\!\rangle$ is the initial vacuum state, the double bars and brackets are used to indicate that this is a state of the second-quantised quantum field theory [27]. After some operator algebra and using the commutator relations $[\hat{b}_p, \hat{b}_{p'}^{\dagger}]_+ = \delta_{p,p'}$ $[\hat{d}_n, \hat{d}_{n'}^{\dagger}]_+ = \delta_{n,n'}$, the total EPP number can be expressed through the energy eigenstates of the field-free Hamiltonian

$$N(t) = \sum_{p,n} |\langle p|U(t)|n\rangle|^2, \quad (6)$$

where the usual quantum mechanical states are denoted by a single bar and bracket. The time evolution operator $U(t) = \hat{T}\exp[-i\int_0^t h(t')dt']$ evolves the initial negative state $|n\rangle$ follows the single-particle Dirac equation. The total time evolution from 0 to t_{max} is divided into N_T intervals, $\Delta t = t_{\mathrm{max}}/N_T$ with an order of 10^{-6}a.u. The time evolution operator in each time step can be written as

$$U(t + \Delta t, t)$$
$$= \hat{T}\exp\left[-i\int_t^{t+\Delta t}(h_0 + V(x, t))dt\right]$$
$$= \exp\left[-i\int_t^{t+\Delta t}\frac{V(x, t)}{2}dt\right] \times \exp\left[-i\int_t^{t+\Delta t}h_0 dt\right]$$
$$\times \exp\left[-i\int_t^{t+\Delta t}\frac{V(x, t)}{2}dt\right] + O(\Delta t^3)$$
$$\simeq \exp\left(\frac{-iV\Delta t}{2}\right)\exp(-ih_0\Delta t)\exp\left(\frac{-iV\Delta t}{2}\right) + O(\Delta t^3). \quad (7)$$

This is the split operator technique based on the third-order algorithm [25,30–32]. Applying the fast Fourier transformation between the spatial and momentum space, the time evolution operator is decomposed into N_T consecutive actions. The time-evolved state $|n(t)\rangle = U(t)|n\rangle$ can be obtained, and then the total EPP number $N(t)$ can be calculated out.
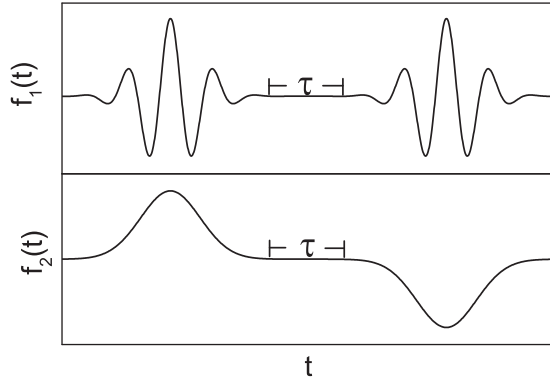
FIG. 1. The temporal schematic picture of the double cosine-Gaussian pulse (top) and the alternating-sign double-Gaussian pulse (bottom).

The external field represented by the scalar potential is $V_i(x,t) = V(x)f_i(t)(i = 1, 2)$, where $f_i(t)$ is the temporal distribution and $V(x) = V[1 + \tanh((x - x_0)/W)]/2$ is the spatial distribution, which indicates that the electric pulse is confined in a range of about $2W$ along the x direction. The double cosine-Gaussian pulse $[V_1(x,t)]$ and the alternating-sign double-Gaussian pulse $[V_2(x,t)]$ are both combined by two sequential pulses, with a time interval between the first and the second pulses. The spatial distribution of the first pulse and the second pulse are $V(x)$. Furthermore, $f_1(t)$ and $f_2(t)$ are as follows:

$$f_1(t) = \begin{cases} e^{-(t-t_{01})^2/2T_1^2} & \cos[\omega(t - t_{01}) + \chi_1] \\ & \qquad\qquad 0 < t < 2t_{01} \\ 0 & 2t_{01} \leqslant t \leqslant 2t_{01} + \tau, \\ e^{-(t-t_{02})^2/2T_2^2} & \cos[\omega(t - t_{02}) + \chi_2] \\ & \qquad\qquad 2t_{01} + \tau < t < t_{max} \end{cases} \quad (8)$$

$$f_2(t) = \begin{cases} e^{-(t-t_{01})^2/2T_1^2} & 0 < t < 2t_{01} \\ 0 & 2t_{01} \leqslant t \leqslant 2t_{01} + \tau, \\ -e^{-(t-t_{02})^2/2T_2^2} & 2t_{01} + \tau < t < t_{max} \end{cases} \quad (9)$$

where T_1 and T_2 are the pulse durations, and τ is the time interval. V is the pulse strength, and in our model the strength of the first pulse and the second pulse are the same. Furthermore, in the double cosine-Gaussian pulse, ω is the carrier frequency, and $\sigma = \omega T_i (i = 1, 2)$ is the number of the oscillation cycles within the Gaussian envelope. χ_1 and χ_2 are the CEP of the first pulse and the second pulse, respectively. In our simulations, $t_{max} = 0.003$ a.u. The schematics of $f_1(t)$ and $f_2(t)$ are shown in Fig. 1.

III. RESULTS AND DISCUSSION

We study the dependence of the total EPP number(N) on the time interval (τ) for both of the symmetric $(T_1 = T_2)$ and the asymmetric $(T_1 \neq T_2)$ cases of $V_1(x,t)$ and $V_2(x,t)$. Finally, the dependence of the total EPP number on the time interval under the double-Gaussian pulse with the same sign is studied as well. For all of the field configurations, the effects of the pulse parameters on the $N(\tau)$ curve are discussed as

TABLE I. Values of pulse parameters.

Pulse parameter	Parameter value		
$\chi\,(\chi_1\ \chi_2)$[a]	0	$\pi/4$	
V	$1.5c^2$	$2c^2$	
$T\,(T_1\ T_2)$	$\dfrac{1}{2\sqrt{2}c^2}$	$\dfrac{1}{\sqrt{2}c^2}$	$\dfrac{2}{\sqrt{2}c^2}$

[a]χ_1 and χ_2 only for cosine-Gaussian pulse.

well. The parameter values that will be used in the following studies are listed in Table I. Under these pulse parameters, the Keldysh parameter $\gamma = mc\omega/qE \gg 1$, then the EPP creation is in the multiphoton regime.

A. Double cosine-Gaussian pulse

In the double cosine-Gaussian pulse, the EPP creation process depends on the pulse parameters, since the pulse strength influences the photon density, the pulse duration determines the number of cycles, and the CEP influences the turning points. We study the dependence of the total EPP number on the time interval for various pulse parameters. The symmetric case is studied first. The dependence of the total EPP number on the time interval under three sets of pulse strength and pulse duration are shown in Fig. 2, when the CEP of the two pulses are zero. Furthermore, the numerical data results are fitted by a fitting formula.

As shown in Fig. 2, the dependencies of the total EPP number on the time interval are almost exactly consistent with the fitting formula Eq. (10) for different pulse strengths and durations. The total EPP number oscillates at a constant period, and its amplitude decays exponentially with the time interval. The oscillation frequencies for all of the cases are about $2c^2$ ($\omega_{Na} = \omega_{Nb} = \omega_{Nc} = 2.01c^2$). Concerning the effects of the pulse strength and the pulse duration, on one hand, the larger pulse strength brings a higher photon density, which
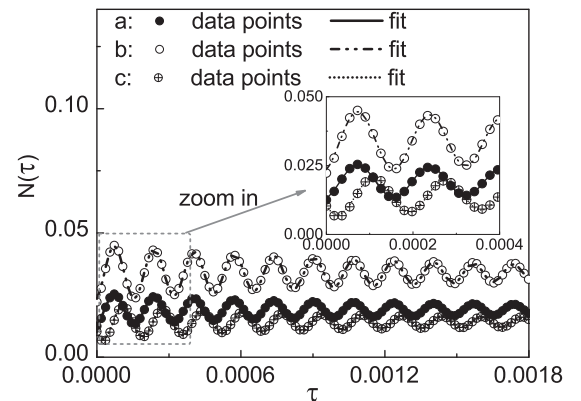

FIG. 2. The evolution of $N(t = 0.003$ a.u.$)$ with τ in the symmetric double cosine-Gaussian pulse. Three sets of pulse strength and the pulse duration are chosen: (curve a) $T_1 = T_2 = 1/\sqrt{2}c^2$, $V = 1.5c^2$, (curve b) $T_1 = T_2 = 1/\sqrt{2}c^2$, $V = 2c^2$, and (curve c) $T_1 = T_2 = 1/2\sqrt{2}c^2$, $V = 2c^2$. Furthermore, $\omega = 2\sqrt{2}c^2$, $\chi_1 = \chi_2 = 0$, $m = 1$ a.u., and $W = 3/c$. The inset is the amplification of the results from $\tau = 0$ a.u. to $\tau = 0.0004$ a.u.

can enhance the EPP creation probability. Comparing curve a with curve b, the amplitude of the total EPP number in curve b is larger than that in curve a, this is consistent with our analysis. Furthermore, the peaks and valleys in curve a and curve b correspond one-to-one. This indicates that the phase of the $N(\tau)$ curve is independent of the pulse strength. On the other hand, in the double-slit picture, the finite pulse duration corresponds to a certain number of oscillation cycles, i.e., $\sigma = \omega T$. The σ cycles of each pulse correspond to σ slit. Besides, the range of the frequency spectrum centered on the carrier frequency decreases (increases) as the pulse duration increases (decreases), which maybe affect the multiphoton process [33]. Therefore the effects of the pulse duration on the EPP creation are complicated. Comparing curve c with curve b, the change of the duration affects both the amplitude and the phase of the $N(\tau)$ curve.

The oscillation of the total EPP number is analogous to the oscillation of the superconductor order parameter detected by the pump-probe pulse. The order parameter damply oscillates with the time interval (time delay between the pump pulse and the probe pulse), and the oscillation frequency equals to twice of the superconductor gap ($2\Delta_0$) [34,35]. Additionally, the Dirac vacuum and the BCS superconductor have more similarities in nature. The Dirac vacuum [36] and the BCS superconductor ground state [37,38] are particle-hole symmetry, i.e., the negative energy eigenstates are all filled with electrons in the Dirac vacuum (or cooper pairs in the BCS superconductor ground state), and the negative energy eigenstates are all empty, with a energy gap between the positive continuum and the negative continuum. The Hamiltonian of the BCS ground state $H_{\mathrm{BCS}} = \epsilon_p \sigma_3 + \Delta_0 \sigma_1$ and the Hamiltonian of the Dirac vacuum $H_D = cp\sigma_1 + mc^2\sigma_3$. H_{BCS} and H_D have a one-to-one correspondence by applying a unitary transformation $U^+ H_{\mathrm{BCS}} U = \epsilon_p \sigma_1 + \Delta_0 \sigma_3$, unitary matrix U can be chosen as $1/\sqrt{2}(\sigma_1 + \sigma_3)$. Therefore the particle creation from the Dirac vacuum and the BCS superconductors are governed by the same equation [39]. A famous quote said by R.Feynman is that "the same equations have the same solutions," then the same phenomenon can occur in different but similar systems, e.g., the Sauter-Schwinger effect originating from the QED can occur in materials governed by the same (Dirac) Hamiltonian [40]. Due to the various similarities between the BCS superconductor and the Dirac vacuum, the fitting formula for the oscillation of the total EPP number is referred to the formula of the damp oscillation of the BCS superconductor order parameter. The formula fitted the total EPP number is

$$N(\tau) = D \exp(-\beta\tau) \sin(\omega_N \tau + \phi) + N_{\mathrm{inf}}, \quad (10)$$

here D is the amplitude, β is the decay factor, ω_N is the oscillation frequency, ϕ is the phase of the $N(\tau)$ curve, and N_{inf} is the asymptotic total created pair numbers at the long time limit.

The CEP is an important parameter in few-cycle short pulse, since it can influence the EPP creation probability or the momentum distribution by changing the distribution of the turning points [6,7]. The dependence of the total EPP number on the time interval for four sets of pulse CEPs are shown in Fig. 3, when the pulse strength and the pulse duration are
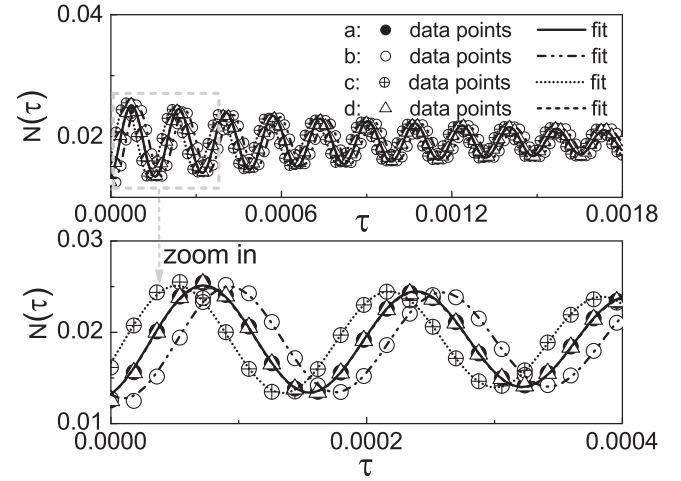
FIG. 3. The evolution of $N(t = 0.003$ a.u.$)$ with τ in the symmetric double cosine-Gaussian pulse. Four sets of CEP of the first pulse and the second pulse are chosen: (curve a) $\chi_1 = \chi_2 = 0$, (curve b) $\chi_1 = 0$, $\chi_2 = \pi/4$, (curve c) $\chi_1 = \pi/4$, $\chi_2 = 0$, and (curve d) $\chi_1 = \pi/4$, $\chi_2 = \pi/4$. Furthermore, $V = 1.5c^2$, $T_1 = T_2 = 1/\sqrt{2}c^2$, $\omega = 2\sqrt{2}c^2$, $m = 1$ a.u., and $W = 3/c$. The bottom picture is the amplification of the results from $t = 0$ to 0.0004 a.u.

fixed. The dependencies of the total EPP number with the time interval are almost exactly consistent with Eq. (10) for all of the cases. The oscillation frequencies of the $N(\tau)$ curves are about $2c^2$ ($\omega_{Na} = \omega_{Nb} = \omega_{Nc} = \omega_{Nd} = 2.01c^2$). As for the effect of the CEP, we find that the CEP advance of the first pulse causes the phase advance of the $N(\tau)$ curve (e.g., $\phi_c - \phi_a \approx \pi/4$), the CEP advance of the second pulse causes a phase lag of the $N(\tau)$ curve (e.g. $\phi_b - \phi_a \approx -\pi/4$). the phase advance (or lag) of the $N(\tau)$ curve is equal to the nonzero CEP, when the CEP of one of the two pulses is nonzero. However, when the CEP of the two pulses are both nonzero, the phase change of the $N(\tau)$ curve is the superposition of the CEP effects brought by the two pulses. Especially, if the CEP of the two pulses are nonzero and the same, the phase of the $N(\tau)$ curve is finally unchanged (e.g., $\phi_d = \phi_a = 1.196$). Furthermore, the CEP of the pulse just affects the phase and does not affect the amplitude of the total EPP number.

The symmetric case of the double cosine-Gaussian pulse is studied above. Then we study the asymmetric case. The dependence of the total EPP number on the time interval is shown in Fig. 4 for three sets of pulse parameters (pulse strength and the first pulse duration), while the second pulse duration is fixed and the CEP of the two pulses are zero. The dependencies of the total EPP number on the time interval are also almost exactly consistent with the fitting formula Eq. (10) for all of the cases. Furthermore, the oscillation frequencies of the $N(\tau)$ curves are about $2c^2 (\omega_{Na} = \omega_{Nb} = \omega_{Nc} = 2.01c^2)$. As for the effects of the pulse strength and the pulse duration, the increase of the pulse strength V enhances the amplitude, but does not affect the phase of the $N(\tau)$ curve, comparing curve a with curve b. The duration of the first pulse affects both the amplitude and the phase of the $N(\tau)$ cure, comparing curve b with curve c. Therefore the effects of the pulse
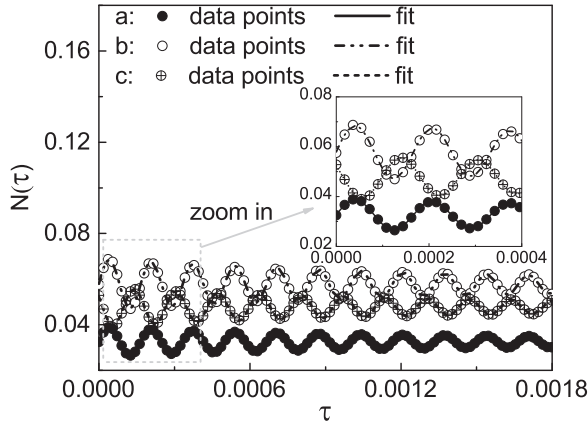
FIG. 4. The evolution of $N(t=0.003$ a.u.) with τ in the asymmetric double cosine-Gaussian pulse. Three sets of pulse strength and the first pulse duration are chosen: (curve a) $T_1 = 1/\sqrt{2}c^2$, $V = 1.5c^2$, (curve b) $T_1 = 1/\sqrt{2}c^2$, $V = 2c^2$, and (curve c) $T_1 = 1/2\sqrt{2}c^2$, $V = 2c^2$. Furthermore, $T_2 = 2/\sqrt{2}c^2$, $\omega = 2\sqrt{2}c^2$, $\chi_1 = \chi_2 = 0$, $m = 1$ a.u., and $W = 3/c$. The inset is the amplification of the results from $\tau = 0$ to 0.0004 a.u.

strength and the pulse duration are the same as the findings obtained in the symmetric case.

Subsequently, we study the effects of the CEP and the pulse sequence swap on the $N(\tau)$ curve. The dependencies of the total EPP number on the time interval for four sets of pulse CEPs are shown in Fig. 5, when the pulse strength and the pulse duration are fixed. Furthermore, the results after swapping the pulse sequence in each of the four cases are studied as well. The dep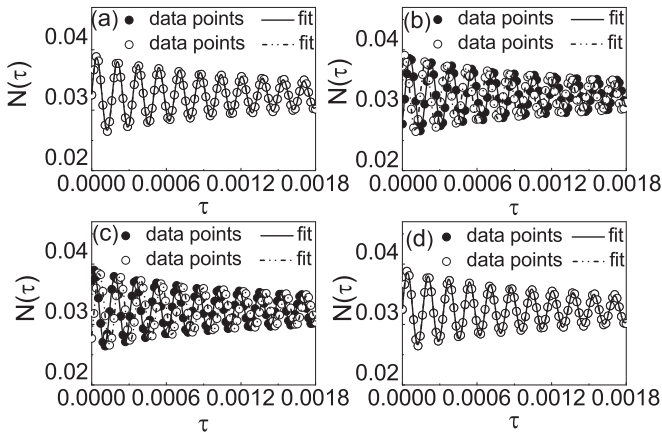endencies of the total EPP number on the time interval almost exactly follow the fitting formula for all of the cases, and the oscillation frequencies are about $2c^2$ [the fitted results of the $N(\tau)$ curves are $2.01c^2$]. The phases of the $N(\tau)$ curves in Fig. 5 are fitted as follows: $\phi_a = 0.033$, $\phi_{bs} = -0.76$ $\phi_{bh} = 0.82$ (s represents solid dot and h represents hollow dot), $\phi_{cs} = 0.82$ $\phi_{ch} = -0.75$, $\phi_d = 0.033$. As for the effect of the CEP, the phase advance of the first pulse causes the phase advance of the $N(\tau)$ curve (e.g., $\phi_{bh} - \phi_a$ and $\phi_{cs} - \phi_a$ are about $\pi/4$), while the CEP effect brought by the second pulse is opposite (e.g., $\phi_{bs} - \phi_a$ and $\phi_{ch} - \phi_a$ are about $-\pi/4$). The phase advance (or lag) of the $N(\tau)$ curve is equal to the nonzero CEP, when the CEP of one of the two pulses is nonzero. Furthermore, when the CEP of the two pulses are both nonzero, the phase change of the $N(\tau)$ curve is the superposition of the CEP effect brought by the two pulses, e.g., $\phi_d = \phi_a$. Therefore the effect of the CEP in the asymmetric case is the same as that in the symmetric case. On the other hand, swapping the pulse sequence does not influence the $N(\tau)$ curve at all when the CEP of the two pulse are the same, as shown in Figs. 5(a) and 5(d). However, when the CEP of the two pulses are different, swapping the sequence affects the phase, but does not affect the amplitude of the $N(\tau)$ curve. This is because the effect of χ_1 and χ_2 on the phase of the $N(\tau)$ curve are opposite. The final phase change of the $N(\tau)$ curve is the superposition of the CEP effect brought by the two pulses. The swapping of the pulse sequence causes the exchange of χ_1 and χ_2, so that the final phase of the $N(\tau)$ curve are different before and after the pulse sequence is swapped. As shown in Figs. 5(b) and 5(c), the phase difference is $\pi/2$ between the $N(\tau)$ curve before and after the pulse sequence is swapped.

B. Alternating-sign double-Gaussian pulse

Since the EPP creation is sensitive to the temporal pulse shape, the alternating-sign double-Gaussian pulse is applied to the vacuum in this section. Different from the cosine-Gaussian pulse, the Gaussian pulse is a monocycle pulse. Subsequently, the symmetric ($T_1 = T_2$) case is studied first. The dependence of the total EPP number on the time interval for three sets of pulse strength and pulse duration are shown in Fig. 6.

In Fig. 6, the total EPP number damply oscillates with the time interval for all of the cases, and the oscillations are also almost exactly consistent with the fitting formula (10). The oscillation frequencies for all of the cases are about $2c^2$ ($\omega_{Na} = \omega_{Nb} = \omega_{Nc} = 2.01c^2$). The increase of the pulse strength can increase the photon density, which can enhance the EPP creation probability. Comparing curve a with curve b, the increase of the pulse strength enhances the amplitude, but does not affect the phase of the $N(\tau)$ curve. The increase (or decrease) of the pulse duration can decrease (or increase) the frequency spectrum of the photons. This can affect the multiphoton EPP creation process. Comparing curve b with curve c, the pulse duration affects both the amplitude and the phase of the $N(\tau)$ curve.

In the asymmetric case, the durations of the two pulses are different. The dependence of the total EPP number on the time interval are studied for three sets of pulse parameters, in which the second pulse duration T_2 is fixed. Furthermore, the situation after the pulse sequence is swapped in theses
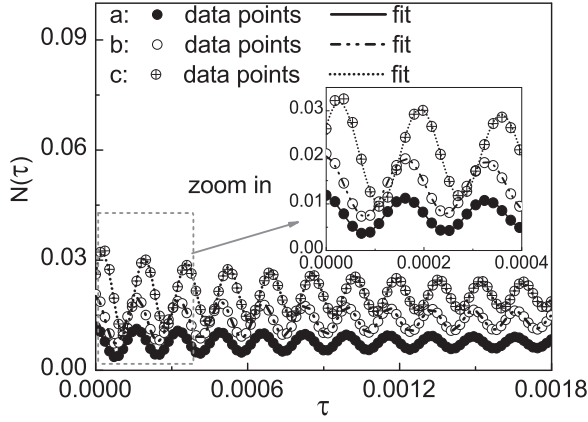

FIG. 5. The evolution of $N(t=0.003$ a.u.) with τ in the asymmetric double cosine-Gaussian pulse. The pulse strength is $V=1.5c^2$. Eight sets of pulse duration and CEP are chosen: (a) solid dot: $T_1 = 1/\sqrt{2}c^2$, $T_2 = 2/\sqrt{2}c^2$, $\chi_1 = \chi_2 = 0$; and hollow dot: $T_1 = 2/\sqrt{2}c^2$, $T_2 = 1/\sqrt{2}c^2$, $\chi_1 = \chi_2 = 0$, (b) solid dot: $T_1 = 1/\sqrt{2}c^2$, $\chi_1 = 0$, $T_2 = 2/\sqrt{2}c^2$, $\chi_2 = \pi/4$; and hollow dot $T_1 = 2/\sqrt{2}c^2$, $\chi_1 = \pi/4$, $T_2 = 1/\sqrt{2}c^2$, $\chi_2 = 0$, (c) solid dot: $T_1 = 1/\sqrt{2}c^2$, $\chi_1 = \pi/4$, $T_2 = 2/\sqrt{2}c^2$, $\chi_2 = 0$; and hollow dot $T_1 = 2/\sqrt{2}c^2$, $\chi_1 = 0$, $T_2 = 1/\sqrt{2}c^2$, $\chi_2 = \pi/4$, and (d) solid dot $T_1 = 1/\sqrt{2}c^2$, $T_2 = 2/\sqrt{2}c^2$, $\chi_1 = \chi_2 = \pi/4$; and hollow dot $T_1 = 2/\sqrt{2}c^2$, $T_2 = 1/\sqrt{2}c^2$, $\chi_1 = \chi_2 = \pi/4$. Furthermore, $\omega = 2\sqrt{2}c^2$, $m = 1$ a.u., and $W = 3/c$.

FIG. 6. The evolution of $N(t = 0.003$ a.u.$)$ with τ in the symmetric double-Gaussian pulse. Three sets of pulse strength and the pulse duration are chosen: (curve a) $T_1 = T_2 = 1/\sqrt{2}c^2$, $V = 1.5c^2$, (curve b) $T_1 = T_2 = 1/\sqrt{2}c^2$, $V = 2c^2$, and (curve c) $T_1 = T_2 = 1/2\sqrt{2}c^2$, $V = 2c^2$. Furthermore, $m = 1$ a.u. and $W = 3/c$. The inset is the amplification of the results from $\tau = 0$ to 0.0004 a.u.

three cases is considered as well. As shown in Fig. 7, the dependencies of the total EPP number on the time interval are consistent with the fitting formula Eq. (10) for all of the cases. The oscillation frequencies of the $N(\tau)$ curves are about $2c^2$ ($\omega_{Na} = \omega_{Nb} = \omega_{Nc} = 2.01c^2$). From the detail, the increase of the pulse strength can enhance the amplitude, and does not affect the phase of the $N(\tau)$ curve, comparing curve a with curve b. The pulse duration affects both the amplitude and the phase of the $N(\tau)$ curve. Furthermore, the results before and after swapping the pulse sequence completely coincide.

C. Double-Gaussian pulse with the same sign

The double cosine-Gaussian pulse and the alternating-sign double-Gaussian pulse both contain conjugate turning points, which can lead to the Ramsey interference effect in the EPP creation [6,12,14–16]. Subsequently, we investigate whether the interference effect is responsible for the damp oscillation of the total EPP number with the time interval. The double-Gaussian pulse with the same signs is applied (i.e., the sign before the exponential function is positive in the second pulse of $f_2(t)$), which does not have two conjugate turning points and then the interference effect is absent [12].
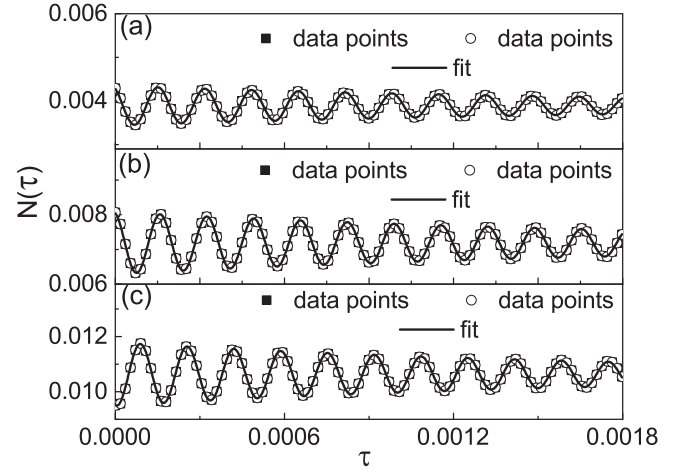

FIG. 7. The evolution of $N(t = 0.003$ a.u.$)$ with τ in the asymmetric double-Gaussian pulse. Six sets of pulse strength and the pulse duration are chosen: (a) solid square: $T_1 = 1/\sqrt{2}c^2$, $T_2 = 2/\sqrt{2}c^2$, $V = 1.5c^2$; and hollow dot: $T_1 = 2/\sqrt{2}c^2$, $T_2 = 1/\sqrt{2}c^2$, $V = 1.5c^2$, (b) solid square: $T_1 = 1/\sqrt{2}c^2$, $T_2 = 2/\sqrt{2}c^2$, $V = 2c^2$; and hollow dot: $T_1 = 2/\sqrt{2}c^2$, $T_2 = 1/\sqrt{2}c^2$, $V = 2c^2$, and (c) solid square: $T_1 = 1/2\sqrt{2}c^2$, $T_2 = 2/\sqrt{2}c^2$, $V = 2c^2$; and hollow dot: $T_1 = 2/\sqrt{2}c^2$, $T_2 = 1/2\sqrt{2}c^2$, $V = 2c^2$. Furthermore, $m = 1$ a.u. and $W = 3/c$.

The dependence of the total EPP number on the time interval for the same-sign and the alternating-sign double-Gaussian pulse are shown in Fig. 8.

In the same-sign double-Gaussian pulse, the dependence of the total EPP number on the time interval are consistent with the fitting formula as well. Compared with the alternating-sign double-Gaussian pulse, the $N(\tau)$ curve between them only has a phase difference of π. The results indicate that the characteristic oscillation still exists even without the interference effect. Therefore, the characteristic oscillation of the total EPP number is not resulted from the interference effect caused by the conjugate turning points.

For all of the studied cases, the evolution of the total EPP number with the time interval is consistent with Eq. (10), which can describe the oscillation of the order parameter in the BCS superconductor as well. The superconductor order parameter damply oscillates with the time interval, and the oscillation frequency is twice of the superconductor gap, detected by the pump-probe technique. This phenomenon is

TABLE II. Similarities between the BCS superconductor and the Dirac vacuum.

	Dirac vacuum	BCS superconductor ground state
Hamiltonian	$H_D = cp\sigma_1 + mc^2\sigma_3$	$H_{BCS} = \epsilon_p\sigma_3 + \Delta_0\sigma_1$[a]
Energy spectrum	$E = \pm\sqrt{c^2p^2 + m^2c^4}$	$E = \pm\sqrt{\epsilon_p^2 + \Delta_0^2}$
Energy gap	$2mc^2$	$2\Delta_0$
Studied quantity	N(total EPP number)	Δ (order parameter)
External field	double pulse (time interval τ)	pump-probe pulse (time interval τ)
phenomenon	$N(\tau)$ damp oscillation (frequency $2mc^2$)	$\Delta(\tau)$ damp oscillation (frequency $2\Delta_0$)

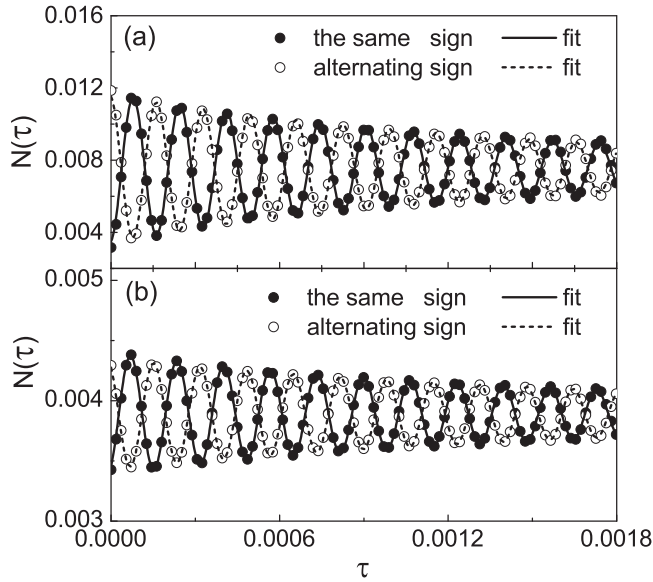[a]ϵ_p is the kinetic energy for single electron, Δ_0 is the superconductor gap.

FIG. 8. The evolution of $N(t = 0.003$ a.u.) with τ in the alternating-sign and identical-sign double-Gaussian pulse. Four sets of double-Gaussian pulse are studied: (a) $T_1 = T_2 = 1/\sqrt{2}c^2$, $V = 1.5c^2$ for both the alternating-sign (hollow dot) and the same-sign (solid dot) double Gaussian pulse, (b) $T_1 = 1/\sqrt{2}c^2$, $T_2 = 2/\sqrt{2}c^2$, $V = 1.5c^2$ for both the alternating-sign (hollow dot) and the same-sign (solid dot) double Gaussian pulse. Furthermore, $m = 1$ a.u. and $W = 3/c$.

proved to be the amplitude mode occurring in the BCS superconductor. We think that the characteristic oscillation of the total EPP number maybe is a manifestation of the amplitude mode excited in the Dirac vacuum, due to the various similarities between the Dirac vacuum and the BCS superconductor. The similarities are summarized in Table II.

D. The comparison with the single pulse

Finally, we make a comparison between the pair creation in the double pulse and two single pulses. Each single pulse respectively corresponds to the first pulse and the second pulse of the double pulse. The relation between N_{inf} and N_s is studied, where N_{inf} is the asymptotic value of $N(\tau)$ when $\tau \to \infty$, N_s is the final total EPP number when the action of the single pulse is finished. Values of N_{inf} and N_s for several

cases are listed in Table III, in which the strength $V = 1.5c^2$ for all of the pulses.

For all of the cases, N_{inf} is equal to the sum of N_s obtained in each single pulse. As studied above, the total EPP number damply oscillates around the value of N_{inf} when the time interval changes. The good value of the time interval can make the EPP number much larger than N_{inf}, i.e., much larger than the sum of the final EPP number created in a single pulse. Therefore the creation of the EPPs can be effectively promoted by adjusting the time interval.

IV. CONCLUSION

To conclude, the dependence of the total EPP number (N) on the time interval (τ) is comprehensively studied under spatially localized double pulse (i.e., the double cosine-Gaussian pulse and the alternating-sign double-Gaussian pulse). The total EPP number damply oscillates with the time interval, and the oscillation is consistent with formula $N(\tau) = D \exp(-\beta\tau) \sin(\omega_N \tau + \phi) + N_{\text{inf}}$ for all of the cases. From the details, the phase and amplitude of the $N(\tau)$ curve are affected by the pulse parameters. The pulse strength only affects the amplitude of the $N(\tau)$ curve, while the pulse duration affects both the amplitude and the phase of the $N(\tau)$ curve. The effects of the pulse strength and the pulse duration are independent of the temporal pulse shape. In addition, the CEP that exists in the cosine-Gaussian pulses mainly affects the phase of the $N(\tau)$ curve. The CEP advance of the first pulse causes a phase advance of the $N(\tau)$ curve, and the CEP advance of the second pulse causes a phase lag of the $N(\tau)$ curve. The final phase change of the $N(\tau)$ curve is the superimposition of the CEP effects brought by the two pulses. However, the effect of swapping the pulse sequence does depend on the pulse shape. In the monocycle pulse (e.g., double-Gaussian pulse), swapping the pulse sequence does not affect the phase or the amplitude of the $N(\tau)$ curve at all. Nevertheless, in the pulse with subcycle (e.g., double cosine-Gaussian pulse), the effect of swapping the pulse sequence is sensitive to the CEP. If the CEP of the two pulses are different, swapping the pulse sequence mainly affects the phase of the $N(\tau)$ curve. If the CEP of the two pulses are the same, swapping the pulse sequence does not affect the EPP creation.

TABLE III. Relationship between N_{inf} and N_s.

double cosine-Gaussian pulse[a]		single cosine-Gaussian pulse[a]		
$T (T_1, T_2)$	N_{inf}	T	N_s	N_{inf} and N_s
$T_1 = T_2 = 1/\sqrt{2}c^2$	$1.910E-2$	$1/\sqrt{2}c^2$	$9.560E-3$	$N_{\text{inf}} = 2N_s$
$T_1 = 1/\sqrt{2}c^2$	$3.250E-2$	$1/\sqrt{2}c^2$	$9.560E-3 (N_{s1})$	$N_{\text{inf}} = N_{s1} + N_{s2}$
$T_2 = 2/\sqrt{2}c^2$		$2/\sqrt{2}c^2$	$2.296E-2 (N_{s2})$	
double Gaussian pulse		single Gaussian pulse		
$T (T_1, T_2)$	N_{inf}	T	N_s	N_{inf} and N_s
$T_1 = T_2 = 1/\sqrt{2}c^2$	$7.560E-3$	$1/\sqrt{2}c^2$	$3.780E-3$	$N_{\text{inf}} = 2N_s$
$T_1 = 1/\sqrt{2}c^2$	$3.890E-3$	$1/\sqrt{2}c^2$	$3.780E-3 (N_{s1})$	$N_{\text{inf}} = N_{s1} + N_{s2}$
$T_2 = 2/\sqrt{2}c^2$		$2/\sqrt{2}c^2$	$1.072E-4 (N_{s2})$	

[a]CEP is zero in the cosine-Gaussian pulse.

Furthermore, we find that the Ramsey interference effect is not responsible for the characteristic oscillation of the total EPP number with the time interval. The oscillation still exists and is consistent with the fitting formula, when the Ramsey interference effect is absent by applying double-Gaussian pulse with the same signs. Since the evolution of the total EPP number with the time interval are consistent with the fitting formula for all of the cases, the characteristic oscillation maybe has relation with the amplitude mode.

These findings indicate that the EPP creation probability can be enhanced by adjusting the time interval. The proper time delay which corresponds to the peaks in the $N(\tau)$ curve mainly depends on the CEP and the pulse duration. Therefore the time interval should be optimized together with other pulse parameters. This may be helpful for the construction of the experimental scenario.

[1] J. Schwinger, Phys. Rev. **82**, 664 (1951).

[2] D. L. Burke, R. C. Field, G. Horton-Smith, J. E. Spencer, D. Walz, S. C. Berridge, W. M. Bugg, K. Shmakov, A. W. Weidemann, C. Bula, K. T. McDonald, E. J. Prebys, C. Bamber, S. J. Boege, T. Koffas, T. Kotseroglou, A. C. Melissinos, D. D. Meyerhofer, D. A. Reis, and W. Ragg, Phys. Rev. Lett. **79**, 1626 (1997); C. Bamber, S. J. Boege, T. Koffas, T. Kotseroglou, A. C. Melissinos, D. D. Meyerhofer, D. A. Reis, W. Ragg, C. Bula, K. T. McDonald, E. J. Prebys, D. L. Burke, R. C. Field, G. Horton-Smith, J. E. Spencer, D. Walz, S. C. Berridge, W. M. Bugg, K. Shmakov, and A. W. Weidemann, Phys. Rev. D **60**, 092004 (1999).

[3] G. V. Dunne, Eur. Phys. J. D **55**, 327 (2009); A. Ringwald, Phys. Lett. B **510**, 107 (2001); See https://eli-laser.eu; See http://www.xcels.iapras.ru; See http://www.hibef.eu.

[4] K. Krajewska and J. Z. Kamiński, Phys. Rev. A **86**, 052104 (2012); A. I. Titov, H. Takabe, B. Kämpfer, and A. Hosaka, Phys. Rev. Lett. **108**, 240406 (2012); A. Di Piazza, *ibid.* **117**, 213201 (2016).

[5] W. Dittrich and H. Gies, *Probing the Quantum Vacuum* (Springer, Heidelberg, 2000); Y. I. Salamin, S. X. Hu, K. Z. Hatsagortsyan, and C. H. Keitel, Phys. Rep. **427**, 41 (2006).

[6] F. Hebenstreit, R. Alkofer, G. V. Dunne, and H. Gies, Phys. Rev. Lett. **102**, 150404 (2009).

[7] C. K. Dumlu, Phys. Rev. D **82**, 045007 (2010).

[8] N. Abdukerim, Z. L. Li, and B. S. Xie, Phys. Lett. B **726**, 820 (2013).

[9] F. Fillion-Gourdeau, F. Hebenstreit, D. Gagnon, and S. MacLean, Phys. Rev. D **96**, 016012 (2017).

[10] X. X. Zhou, C. K. Li, M. Jiang, N. S. Lin, and Y. J. Li, Europhys. Lett. **128**, 10001 (2019).

[11] R. Schützhold, H. Gies, and G. Dunne, Phys. Rev. Lett. **101**, 130404 (2008); C. Schneider and R. Schützhold, Phys. Rev. D **94**, 085015 (2016); G. Torgrimsson, C. Schneider, J. Oertel, and R. Schützhold, J. High Energ. Phys. 06 (2017) 043.

[12] E. Akkermans and G. V. Dunne, Phys. Rev. Lett. **108**, 030401 (2012).

[13] F. Hebenstreit and F. Fillion-Gourdeau, Phys. Lett. B **739**, 189 (2014).

[14] M. J. A. Jansen and C. Müller, Phys. Lett. B **766**, 71 (2017).

[15] L. F. Granz, O. Mathiak, S. Villalba-Chávez, and C. Müller, Phys. Lett. B **793**, 85 (2019).

[16] A. Ilderton, Phys. Rev. D **101**, 016006 (2020).

[17] H. Kleinert, R. Ruffini, and S. S. Xue, Phys. Rev. D **78**, 025011 (2008); Q. Z. Lv, J. Unger, Y. T. Li, Q. Su, and R. Grobe, Europhys. Lett. **116**, 40003 (2016); S. S. Dong, M. Chen, Q. Su, and R. Grobe, Phys. Rev. A **96**, 032120 (2017).

[18] T. Heinzl, A. Ilderton, and M. Marklund, Phys. Lett. B **692**, 250 (2010).

[19] C. K. Dumlu and G. V. Dunne, Phys. Rev. D **83**, 065028 (2011).

[20] C. Fey and R. Schützhold, Phys. Rev. D **85**, 025004 (2012).

[21] F. Sauter, Z. Physik **69**, 742 (1931).

[22] A. Hansen and F. Ravndal, Phys. Scr. **23**, 1036 (1981).

[23] B. Thaller, *The Dirac Equation* (Springer, Berlin, 1992).

[24] K. D. Lamb, C. C. Gerry, Q. Su, and R. Grobe, Phys. Rev. A **75**, 013425 (2007).

[25] J. W. Braun, Q. Su, and R. Grobe, Phys. Rev. A **59**, 604 (1999).

[26] T. Cheng, M. R. Ware, Q. Su, and R. Grobe, Phys. Rev. A **80**, 062105 (2009).

[27] T. Cheng, Q. Su, and R. Grobe, Contemp. Phys. **51**, 315 (2010).

[28] W. Greiner, B. Müller, and J. Rafelski, *Quantum Electrodynamics of Strong Fields* (Springer-Verlag, Berlin, 1985), See Eq. (9.9) in Chap. 9.

[29] For a review see, e.g., S. S. Schweber, *An Introduction to Relativistic Quantum Field Theory* (Harper & Row, New York, 1962).

[30] A. D. Bandrauk and H. Shen, J. Phys. A **27**, 7147 (1994).

[31] G. R. Mocken and C. H. Keitel, Comput. Phys. Commun. **178**, 868 (2008).

[32] M. Ruf, H. Bauke, and C. H. Keitel, J. Comput. Phys. **228**, 9092 (2009).

[33] V. S. Popov, Sov. Phys. JETP **34**, 709 (1972).

[34] Y. Murakami, P. Werner, N. Tsuji, and H. Aoki, Phys. Rev. B **94**, 115126 (2016).

[35] R. Matsunaga, Y. I. Hamada, K. Makise, Y. Uzawa, H. Terai, Z. Wang, and R. Shimano, Phys. Rev. Lett. **111**, 057002 (2013).

[36] P. A. M. Dirac, Proc. R. Soc. London, Ser. A **117**, 610 (1928).

[37] J. Bardeen, L. N. Cooper, and J. R. Schrieffer, Phys. Rev. **108**, 1175 (1957).

[38] N. N. Bogoljubov, V. V. Tolmachov, and D. V. Širkov, Fortschr. Phys. **6**, 605 (1958).

[39] Y. Nambu and G. Jona-Lasinio, Phys. Rev. **122**, 345 (1961); D. Pekker and C. M. Varma, Annu. Rev. Condens. Matter Phys. **6**, 269 (2015).

[40] D. Allor, T. D. Cohen, and D. A. McGady, Phys. Rev. D **78**, 096009 (2008); M. F. Linder, A. Lorke, and R. Schützhold, Phys. Rev. B **97**, 035203 (2018).